

# The Role of Properdin in Zymosan- and *Escherichia coli*-Induced Complement Activation

Morten Harboe,\* Peter Garred,<sup>†</sup> Julie K. Lindstad,\* Anne Pharo,\* Fredrik Müller,<sup>‡</sup> Gregory L. Stahl,<sup>§</sup> John D. Lambris,<sup>¶</sup> and Tom E. Mollnes\*

Properdin is well known as an enhancer of the alternative complement amplification loop when C3 is activated, whereas its role as a recognition molecule of exogenous pathogen-associated molecular patterns and initiator of complement activation is less understood. We therefore studied the role of properdin in activation of complement in normal human serum by zymosan and various *Escherichia coli* strains. In ELISA, microtiter plates coated with zymosan induced efficient complement activation with deposition of C4b and terminal complement complex on the solid phase. Virtually no deposition of C4b or terminal complement complex was observed with mannose-binding lectin (MBL)-deficient serum. Reconstitution with purified MBL showed distinct activation in both readouts. In ELISA, normal human serum-induced deposition of properdin by zymosan was abolished by the C3-inhibiting peptide compstatin. Flow cytometry was used to further explore whether properdin acts as an initial recognition molecule reacting directly with zymosan and three *E. coli* strains. Experiments reported by other authors were made with EGTA Mg<sup>2+</sup> buffer, permitting autoactivation of C3. We found inhibition by compstatin on these substrates, indicating that properdin deposition depended on initial C3b deposition followed by properdin in a second step. Properdin released from human polymorphonuclear cells stimulated with PMA did not bind to zymosan or *E. coli*, but when incubated in properdin-depleted serum this form of properdin bound efficiently to both substrates in a strictly C3-dependent manner, as the binding was abolished by compstatin. Collectively, these data indicate that properdin in serum as well as polymorphonuclear-released properdin is unable to bind and initiate direct alternative pathway activation on these substrates. *The Journal of Immunology*, 2012, 189: 2606–2613.

Zymosan, which is a carbohydrate complex derived from yeast cell walls, is an essential reagent in studies of complement activation. Pillemer et al. (1) first described properdin, providing evidence that zymosan/properdin complexes induced Ab-independent complement activation (2). Reaction between properdin and various bacterial polysaccharides was also reported. The findings were controversial at that time, difficult to reproduce, and with Pillemer's death (3–5) properdin was largely dismissed by the scientific community. The properdin system was reborn as the alternative pathway (AP) >20 y later (2, 4). Properdin is now denoted factor P (fP), and the current description of

two different functions of fP (2, 6–9) has been a valuable basis for further studies and development in this area.

In the long-standing model, AP is slowly autoactivated by hydrolysis of C3 with exposure of the internal thioester bond, leading to an initial AP convertase that cleaves C3, and C3b is subsequently covalently attached to nearby targets. Bound C3b then binds to iB, which is cleaved by factor D (fD). The Ba fragment is released into the fluid phase. Bb remains as part of the C3bBb complex, the potent AP C3 convertase, which splits more C3, resulting in self-amplification and generation of the C5 convertase C3bBbC3b. The C3bBb complex is relatively unstable with a half-life of 90 s under physiological conditions (10, 11). fP associates with C3bBb, forming a more stable C3bBbP complex (12, 13) with longer lasting enzyme activity essential for effective AP amplification. Notably, fP is the only known regulator of complement that enhances the activation, whereas all other regulatory proteins have inhibitory properties.

Evidence for the role of fP as a recognition molecule in AP started with experiments showing that purified fP bound to a biosensor surface could serve as a platform for in situ assembly of AP C3 convertases (9, 14). Extensive experiments indicating that AP is initiated by noncovalent attachment of fP to a target surface (2) were, however, performed in EGTA Mg<sup>2+</sup> buffer in which the autoactivation (“tick-over”) of C3 and the AP pathway amplification are intact. Thus, this system would permit continuous C3b deposition, making it difficult to demonstrate whether fP reacts as an initial recognition molecule of zymosan or subsequently binds after C3b deposition. Different reaction patterns of isolated fP, fP in serum, and fP released from activated, degranulated neutrophils are essential in studies of this matter, as pointed out previously (15, 16) and further described in *Results*.

In addition to mannose-binding lectin (MBL), ficolin-1, ficolin-2, and ficolin-3 are recognition units in the lectin pathway (LP) (17–

\*Institute of Immunology, University of Oslo and Oslo University Hospital, Rikshospitalet, NO-0027 Oslo, Norway; <sup>†</sup>Department of Clinical Immunology, Section 7631 Rigshospitalet, Copenhagen University Hospital, DK-2100 Copenhagen Ø, Denmark; <sup>‡</sup>Faculty of Medicine, University of Oslo and Department of Microbiology, Oslo University Hospital, Rikshospitalet, NO-0027 Oslo, Norway; <sup>§</sup>Center for Experimental Therapeutics and Reperfusion Injury, Harvard Medical School, Boston, MA 02115; and <sup>¶</sup>Department of Pathology and Laboratory Medicine, University of Pennsylvania, Philadelphia, PA 19106

Received for publication January 20, 2012. Accepted for publication July 3, 2012.

This work was supported by the Norwegian Research Council, the Norwegian Council on Cardiovascular Disease, the Odd Fellow Foundation, and National Institutes of Health Grants AI068730 and GM60338 (to J.D.L.).

Address correspondence and reprint requests to Prof. Tom Eirik Mollnes, Institute of Immunology, Rikshospitalet University Hospital, N-0027 Oslo, Norway. E-mail address: t.e.mollnes@medisin.uio.no

The online version of this article contains supplemental material.

Abbreviations used in this article: AP, alternative pathway; CP, classical pathway; fD, factor D; fP, factor P; fPd, factor P-depleted; GVB, gelatin veronal buffer; HAIGG, heat-aggregated human IgG; LP, lectin pathway; MBL, mannose-binding lectin; MBLd, mannose-binding lectin-deficient serum; MFI, mean fluorescence intensity; NHP, normal human plasma; NHS, normal human serum; PMN, polymorphonuclear cell; PMNfP, polymorphonuclear cell-released factor P; TCC, terminal complement complex.

Copyright © 2012 by The American Association of Immunologists, Inc. 0022-1767/12/\$16.00

19). Similar to MBL, the ficolins react with *N*-acetylglucosamine, but the fine carbohydrate-binding specificity differs from MBL and they do not react with mannan (19, 20).

Compared with mannan, which has an extensive literature on reactivity and induction of LP activation, in particular that initiated by MBL, less has been reported concerning the mechanisms involved in zymosan-induced LP activation. An early study indicated interaction with proteins later identified as essential constituents of LP (21), whereas formal identification of LP activation by zymosan was first provided by Brouwer et al. (22).

Specific activation of the classical pathway (CP) by heat-aggregated human IgG (HAIGG) has been extensively studied, whereas development of systems for specific activation of LP in close to physiologic conditions has encountered considerable difficulties. However, we have recently developed a system for specific activation of LP without involvement of the CP and with no direct, initial AP activation using mannan coating on the solid phase of ELISA plates and normal human serum (NHS) at high concentration (diluted 1:2) (20). Three main observations indicated LP specificity of this system: 1) mannan on the solid phase induced activation of NHS but not of MBL-deficient serum, showing that MBL is required for the activation; 2) after reconstitution of MBL-deficient serum with purified MBL, activation was obtained, showing that MBL is responsible for activation; and 3) monoclonal anti-MBL Ab 3F8, documented to inhibit MBL function (23), abolished the activation of NHS, showing that activation depends exclusively on MBL.

We have reported that AP amplification contributed to >80% of the final C5a generation after initial HAIGG induced activation highly specific for CP (24). In mannan-induced LP activation, AP amplification has been described by various authors (21, 22). In the system with highly specific LP activation of human whole serum (20), we also found that AP amplification is crucial for the downstream effect of initial LP activation, being responsible for >80% of terminal complement complex (TCC) release into the fluid phase (25).

The purpose of the present study was to apply similar technology to characterize complement activation induced by zymosan and to explore whether fP in NHS as well as fP released from PMA-stimulated polymorphonuclear cells (PMNs) act as an initial recognition molecule reacting directly with zymosan or whole *Escherichia coli*, thereby starting AP activation by itself. To obtain conditions with control of initial C3 activation, we studied the effect of the C3-inhibiting peptide compstatin (26–29) on fP deposition on zymosan and three different strains of “properdin-reactive” *E. coli* strains (2) by flow cytometry. The findings demonstrate that this peptide served to distinguish between initial direct fP binding (30) and secondary fP binding to C3b.

## Materials and Methods

### mAbs

Mouse anti-MBL mAbs 3F8 (IgG1 $\kappa$ ) and 1C10 (IgG2b) were raised by immunization with purified human MBL, reacting with MBL with high affinity. 3F8 reacts with a conformation-dependent epitope in the hinge within the carbohydrate recognition domain of MBL and inhibits MBL-dependent C3 deposition on mannan-coated plates completely at 10  $\mu$ g/ml NHS (23), whereas 1C10 reacts with another epitope, being noninhibiting (31). Mouse anti-human fD (clone 166-32, IgG1 $\kappa$ ) (32) and its isotype-matched control mAb (clone G3-519, anti-HIV gp120, IgG1 $\kappa$ ) were provided by Michael Fung. Inhibiting mouse anti-human fP, clone A233 (IgG1 $\kappa$ ) raised by immunization with purified human fP, was obtained from Quidel (San Diego, CA). Clone IS7 (IgG1 $\kappa$  anti-human CD22) from Diatec Monoclonals (Oslo, Norway) was used as its isotype control. mAb aE11 reacting with a neopeptide exposed when C9 is incorporated in the TCC (33) was obtained from Diatec Monoclonals. Clone 5A7 from Diatec Monoclonals was used as its IgG2a isotype control.

### NHS, plasma, and purified protein and cells

NHS was collected from nine healthy volunteers, all showing normal CP, LP, and AP activity in the Wielisa total complement system screen assay (34). Prior to pooling, the sera were tested for LP activation after exposure to mannan on the solid phase (0.5  $\mu$ g/well) using solid-phase TCC deposition as readout. Activation was obtained and TCC deposition was inhibited completely by 3F8 mAb in all nine sera, excluding interference by CP activation owing to complement-fixing anti-mannan Abs occurring in occasional sera (20, 35). Subsequently, the sera were pooled and stored as aliquots at  $-70^{\circ}\text{C}$ . The MBL concentration of the pool was 740  $\mu$ g/l. To approach physiological conditions in activation assays and to ensure a fully active AP, NHS was used at a final dilution of 1:2, which was the lowest possible dilution to obtain a constant final concentration of serum after addition of buffer and mAbs. Normal human plasma (NHP) was prepared as follows: blood from a healthy volunteer was drawn into an evacuated sterile NUNC plastic tube containing lepirudin (Refludan; Pharmion, Copenhagen, Denmark) to provide 50  $\mu$ g lepirudin/ml blood. After mixing, the tube was centrifuged for 15 min at  $1400 \times g$  at  $4^{\circ}\text{C}$ . The supernatant plasma was divided into aliquots and then frozen at  $-70^{\circ}\text{C}$  for later flow cytometry analysis.

fP-depleted serum (A339 lot 8a) and purified fP (A139 lot 21a) were obtained from Complement Technology (Tyler, TX). fP was quantified by a human properdin ELISA kit (catalog no. HK334) from Hycult Biotech (Uden, The Netherlands) according to the instructions of the manufacturer. Purified plasma-derived MBL was obtained from Statens Serum Institut (Copenhagen, Denmark) (36).

PMNs were isolated by density gradient centrifugation on Polymorphprep (Axis-Shield/Medinor, Oslo, Norway) according to the instructions of the manufacturer, and the cells (a total of  $1 \times 10^8$  cells in a buffer volume of 2.6 ml) were activated by PMA (catalog no. 79346; Sigma-Aldrich, St. Louis, MO) at final concentration of 500 ng/ml in BSA-coated tubes for  $37^{\circ}\text{C}$  for 30 min on a cell roller. The fP concentration in the supernatant after stimulation was quantified in fP ELISA and found to be 6  $\mu$ g/ml.

### Bacteria

*E. coli* strains D31m3, D31m4, and ED3869 were obtained from the *E. coli* Genetic Stock Center at Yale University (New Haven, CT) and cultured on tryptose blood agar base medium (Oxoid, Basingstoke, U.K.) with 2% lactose and 0.5% NaCl, subsequently subcultured in heart infusion broth (Becton Dickinson, Sparks, MD), and harvested during exponential growth before flow cytometry experiments.

### MBL-deficient serum

MBL-deficient serum (MBLd) was selected from an MBL *D/D* (codon 52 variant in the *MBL2* gene) homozygous 35-y-old healthy male with no anti-mannan Abs. The serum had normal CP and AP activity in the Wielisa assay (34) and standard hemolytic assays. It contains dysfunctional low-m.w. MBL that cannot bind ligands or activate the MBL complement system efficiently under physiological conditions (37). Reconstituting the serum with recombinant wild-type MBL has previously shown that the capability of MASP-1/3 and MASP-2 to interact with MBL is normal as well as the capacity to deposit C4 (38).

### Zymosan-induced activation of serum

Zymosan A from *Saccharomyces cerevisiae* (catalog no. Z4250; Sigma-Aldrich, Steinheim, Germany) in a 100  $\mu$ l volume was coated on Costar 3590 flat-bottom polystyrene 96-well plates (Corning, Corning, NY) in 50 mM sodium carbonate buffer (pH 9.6) overnight at room temperature and the fluid was removed. After washing, the remaining binding sites in the wells were saturated with a blocking buffer, PBS (pH 7.4), containing 1% BSA (catalog no. A8327; Sigma-Aldrich, St. Louis, MO) and 0.1% Tween 20 (catalog no. P1379; Sigma-Aldrich, St. Louis, MO) for 1 h at  $37^{\circ}\text{C}$ . After three times washing with PBS containing 0.1% Tween 20, 50  $\mu$ l NHS diluted 1:2 in veronal buffer (pH 7.5) containing 0.5 mM  $\text{MgCl}_2$ , 2 mM  $\text{CaCl}_2$ , 0.05% Tween 20, and 0.1% gelatin (gelatin veronal buffer [GVB]<sup>2+</sup>) was added to each well for complement activation for 30 min at  $37^{\circ}\text{C}$ . To stop LP activation and to ensure complete inhibition of continuing background AP amplification, the microtiter plate was incubated on ice and 10  $\mu$ l EDTA was added immediately to each well to a final concentration of 20 mM before assay for activation products on the solid phase and in the supernatant (fluid phase). Coating with mannan on the solid phase for activation was done in the same way, as reported previously (20).

### Readouts for activation products on the solid phase

Deposition of MBL on the solid phase following activation was demonstrated in ELISA using polyclonal rabbit anti-human MBL2 Ab (1:50; Atlas Abs, Stockholm, Sweden) obtained by immunization with PrEST technology (39, 40) followed by HRP-conjugated donkey anti-rabbit Ig (1:1000; Amersham Biosciences, Little Chalfont, U.K.) with ABTS as substrate. The recombinant peptide used for immunization covered amino acids 102–240 of the MBL sequence (<http://www.atlasantibodies.com>), and antigenicity plot analysis (41) indicated a series of Ab-reactive epitopes in this area.

Deposition of C4b and C3b on the solid phase was demonstrated with polyclonal rabbit anti-human C4 (OSAO 194; 1:10,000) and anti-human C3 (OSAP 192; 1:40,000) Abs (Dade Behring, Marburg, Germany), HRP-conjugated donkey anti-rabbit Ig (1:2,000), and ABTS as substrate.

Deposition of fP on the solid phase in ELISA was with monoclonal anti-fP (Quidel A233; 1:1000) with HRP-conjugated F(ab')<sub>2</sub> anti-mouse IgG (GE Healthcare U.K., Little Chalfont, U.K.; 1:1000) with ABTS as substrate. In inhibition experiments with mAbs, deposition of fP was demonstrated with polyclonal goat anti-human fP (A239; 45 mg/ml; 1:1000) (Complement Technology), HRP-conjugated mouse anti-goat Ig (1:1000; Jackson ImmunoResearch Europe, Newmarket, Suffolk, U.K.) with ABTS as substrate.

Deposition of the TCC was based on reaction with purified mAb aE11 (42) (1 mg/ml [1:6000] in PBS with 0.2% Tween 20) followed by biotin-conjugated rat anti-mouse IgG2a mAb (1:1000; BD Biosciences Pharmingen, Erembodegem, Belgium) and HRP-conjugated streptavidin (1:2000; Amersham Biosciences) with ABTS as substrate, using OD values at 405 nm to represent the relative amount of deposited TCC in the wells.

### Readout for TCC in the fluid phase

TCC in the fluid phase was measured by a double-Ab assay described in detail previously (33, 43). Briefly, mAb aE11 was used as catching Ab, biotinylated anti-C6 mAb 9C4 (43) as detection Ab, HRP-labeled streptavidin (Amersham Biosciences), and ABTS as substrate.

### Inhibition assays

mAbs were added to serum followed by incubation for 5 min at room temperature prior to activation and assay. Optimal concentration was determined in pilot experiments, with control Ab being used in the same amount. The amount of purified mAb per well is recorded as transformed to amount per milliliter of undiluted serum, anti-MBL 3F8 at 20 µg/ml, anti-MBL 1C10 at 20 µg/ml, anti-fD 166-32 at 10 µg/ml, and anti-fP A233 at 20 µg/ml.

The compstatin analog (Ac-I[CV(1MeW)QDWGAHRC]T) with increased C3-inhibiting activity produced as previously described (27, 29) was used at 50 µM.

### Flow cytometry

A FACSCalibur instrument (Becton Dickinson, Franklin Lakes, NJ) was used for flow cytometry with FlowJo analysis software version 7.6.4 (Tree Star, Ashland, OR). Zymosan A (Z-4250; Sigma-Aldrich, Steinheim, Germany) was suspended in PBS with 1% BSA. Blocking was with 1% BSA in PBS (pH 7.4) with 1% Tween 20 for 1 h at 37°C. Subsequent washing at this and all later steps was in PBS with 0.1% BSA. The zymosan was resuspended in GVB<sup>2+</sup>. Incubation with NHS (1:2) was at 37°C for 20 min in GVB<sup>2+</sup> after 5 min preincubation with compstatin at a final concentration of 50 µM. To demonstrate binding of fP, the zymosan was incubated with monoclonal anti-fP (catalog no. A233; Quidel) diluted 1:50 for 15 min at room temperature. The samples were washed twice and further incubated with anti-mouse IgG (Fc specific) FITC-conjugated F(ab')<sub>2</sub> (F2772; Sigma-Aldrich, Steinheim, Germany) diluted 1:50 for 15 min at room temperature in the dark. The samples were washed twice, resuspended in PBS with 1% BSA, and put on ice until analysis in the flow cytometer. Gating was based on forward and side scatter and 20,000 events were acquired. For analysis of *E. coli*, the bacteria were washed and suspended in PBS with 0.1% BSA. Blocking was with 1% BSA in PBS without Tween 20 for 1 h at 20°C. Subsequent washing at this and all later steps was in buffer without Tween 20 to avoid interaction between Tween 20 and lipids in the bacterial surface layer. Incubation with NHS (1:2) was in GVB<sup>2+</sup> at 37°C for 20 min after 5 min preincubation with compstatin at a final concentration of 50 µM. For analysis of TCC binding to *E. coli* the procedures were adjusted to obtain optimal conditions based on the experiments in ELISA. Gating was based on forward and side scatter and 20,000 events were acquired.

### Statistical analysis

GraphPad Prism version 5 (GraphPad Software, San Diego, CA) was used for statistical analyses. Data were examined with ANOVA, by one-way ANOVA followed by the Bonferroni posttest, and by ANOVA with repeated measurements followed by a Dunnett multiple comparison test, and the Student *t* test was used as appropriate for the different experiments. A *p* value <0.05 was considered statistically significant.

### Ethics

The study was approved by the Norwegian Government Regional Committee for Medical Research Ethics.

## Results

### C4b and TCC deposition on zymosan and mannan by NHS and MBL-deficient serum

NHS induced efficient deposition of C4b and TCC on the solid phase in microtiter wells coated with zymosan or with mannan for comparison (Fig. 1), consistent with activation of the whole cascade on both coatings. In contrast, virtually no deposition of C4b or TCC was seen with the MBLd, with a similar result obtained for zymosan and mannan. Reconstitution with purified MBL showed distinct activation with OD values in both readouts comparable to the values for NHS, after addition of 10 µg MBL/ml MBLd. C4b values with MBLd was significantly lower than with NHS and MBLd plus MBL (*p* = 0.0013 and 0.004, respectively) (Fig. 1A). TCC values with MBLd was significantly lower than with NHS and MBLd plus MBL (*p* = 0.004 and 0.0016, respectively) (Fig. 1B). In all sets, the difference of NHS versus

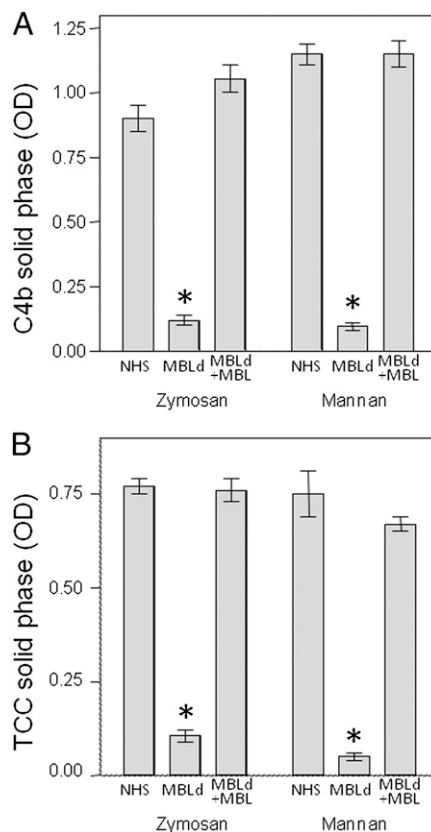


**FIGURE 1.** Reaction pattern of NHS compared with MBLd after activation with zymosan on the solid phase (0.5 µg/well). Reconstitution with 10 µg purified MBL/ml MBLd showed distinct activation with increasing OD values for deposition of C4b and TCC on the solid phase. Data are presented as mean values and range from two independent experiments. On the right, mannan coating on the solid phase (0.5 µg/well) is shown for comparison. Typical findings in four experiments are shown. \**p* < 0.05.



MBLd plus MBL was not significant. Similar observations were made regarding deposition of C3b on the solid phase and release of TCC into the fluid phase (data not shown).

A dose-dependent deposition of C4b on the solid phase was observed after activation of NHS by different amounts of zymosan on the solid phase (Fig. 2A). Addition of the inhibiting anti-MBL mAb 3F8 abolished C4b deposition at all zymosan concentrations, showing OD values similar to the negative buffer control, indicating that no direct, MBL-independent activation leading to C4b deposition occurred in this system. Interference by ficolin-1, -2, and -3 is not expected from recent information on their recognition specificity (19, 44–46). Addition of the noninhibiting mAb 1C10 gave OD values similar to those obtained with NHS alone. The difference between NHS and NHS plus 3F8 was statistically significant ( $p < 0.05$ ), whereas the difference between NHS and NHS plus 1C10 was not significant.

Deposition of MBL on the solid phase after zymosan-induced activation was also completely inhibited with anti-MBL mAb 3F8 (Fig. 2B). The findings concerning statistics were the same as those for Fig. 2A. Control experiments with mannan-induced activation (0.5  $\mu\text{g}/\text{well}$ ) showed the same reaction pattern (in black).

*C3b deposition and TCC formation after zymosan-induced activation and inhibition with anti-MBL*

The dose-dependent NHS mediated C3b deposition on zymosan (Fig. 3A, open circles) was substantially, but not completely, inhibited by anti-MBL mAb 3F8 (Fig. 3A, open squares), similar to the results observed with MBLd (Fig. 3A, filled diamonds), whereas the control anti-MBL mAb 1C10 values (Fig. 3A, open triangles) were similar to NHS. There was a highly significant difference ( $p < 0.0001$ ) between the curves of Fig. 3A. Thus, the differences between NHS and NHS plus 3F8, as well as between NHS and MBLd, were both significant ( $p < 0.05$ ), whereas the difference between NHS and NHS plus 1C10 was not significant. Notably, in a control with mannan on the coat, known to activate only LP in this system (20), the anti-MBL mAb 3F8 completely inhibited C3b deposition (Fig. 3A, filled square), indicating some

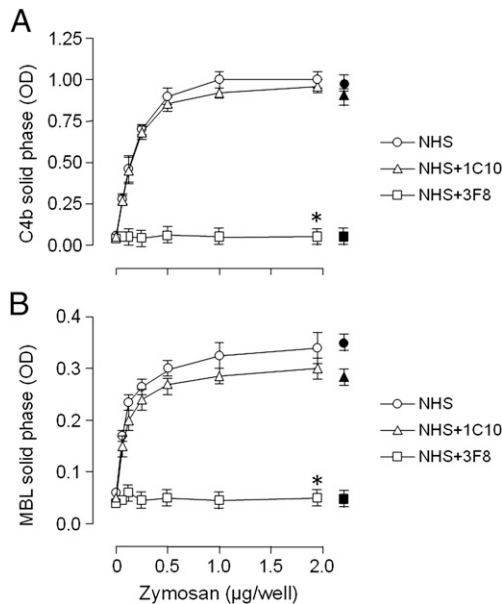


**FIGURE 2.** Deposition of C4b (A) and MBL (B) on the solid phase after activation of NHS by different amounts of zymosan on the solid phase. 3F8 and 1C10 are anti-MBL inhibiting and noninhibiting mAbs, respectively. On the right, in black, mannan coating (0.5  $\mu\text{g}/\text{well}$ ) is shown for comparison. Typical findings in four experiments are shown. \* $p < 0.05$ .

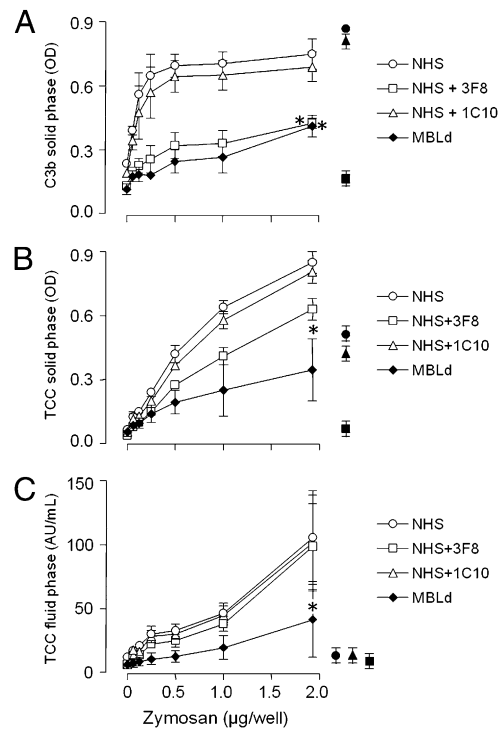


**FIGURE 3.** Deposition of C3b (A) and TCC (B) on the solid phase and release of TCC into the fluid phase (C) after activation of NHS by different amounts of zymosan on the solid phase. Description and data presentation are as in Fig. 2. Typical findings in four experiments are shown. \* $p < 0.05$ .

MBL-independent activation of AP, as judged by C3b deposition, by zymosan but not by mannan.

Data on deposition of TCC on the solid phase (Fig. 3B) showed similarity to deposition of C3b, but with less inhibition by anti-MBL mAb 3F8 on the zymosan coat, whereas the inhibition with anti-MBL mAb 3F8 completely inhibited the activation on mannan, again indicating additional MBL-independent activation of AP by zymosan. There was a highly significant difference between the curves of Fig. 3B ( $p = 0.0035$ ), with MBLd being significantly different from NHS ( $p < 0.05$ ). Release of TCC into the fluid phase showed inhibition by MBLd only ( $p < 0.05$ ) (Fig. 3C).

*Effect of various complement inhibitors on fP deposition on solid-phase zymosan by NHS*

NHS induced a dose-dependent fP deposition on zymosan (Fig. 4A, open circles), which was identical to that seen with the non-inhibitory anti-MBL mAb 1C10 (Fig. 4A, open triangles), whereas anti-MBL mAb 3F8 inhibited the deposition incompletely (Fig. 4A, open squares), similar to what was obtained with anti-fD (open diamonds). In contrast, anti-fP A233 completely abrogated fP deposition (Fig. 4A, inverted open triangles). There was a highly significant difference between the curves of Fig. 4A ( $p < 0.0001$ ), reflected by significances between NHS and NHS plus 3F8 and between NHS and MBLd, as well as between NHS plus anti-fD and NHS plus anti-fP. Notably, in the control with mannan-induced activation specifically activating LP in this system (Fig. 4A, filled symbols), both anti-MBL mAb 3F8 (filled square) and anti-fP (filled inverted triangle) completely inhibited deposition of fP.

In ELISA, deposition of fP on solid-phase zymosan by NHS was completely inhibited by the C3-inhibiting peptide compstatin ( $p = 0.013$ ) (Fig. 4B) in marked contrast to the fully retained deposition of C4b generated earlier in the complement activation cascade ( $p = 0.95$ ) (Fig. 4C).

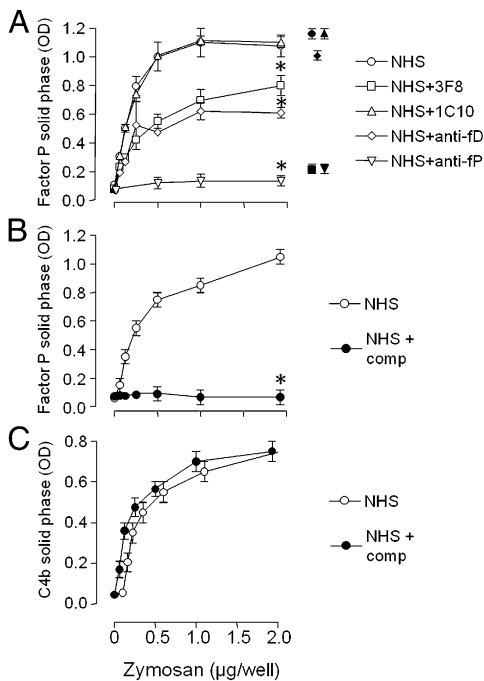


**FIGURE 4.** (A) Inhibition of deposition of fP on the solid phase by anti-MBL, anti-fD (a-fD), and anti-fP (a-fP) mAbs after activation of NHS by different amounts of zymosan on the solid phase. Description and data presentation are as in Fig. 2. Effects of adding compstatin to serum (50  $\mu$ M/ml) on deposition of fP (B) and C4b (C) on the solid phase after activation of NHS by different amounts of zymosan on the solid phase are shown. Typical finding in four experiments are shown. \* $p < 0.05$ .

In separate ELISA experiments, deposition of C3b on solid-phase zymosan by NHS was inhibited significantly ( $p < 0.05$ ) by anti-MBL mAb 3F8, but not by the control anti-MBL mAb 1C10 or by the inhibiting anti-fP mAb A233 or its isotype control (Supplemental Fig. 1). These findings correspond to observations in an earlier study (6) indicating that fP is not essential for zymosan-induced AP complement activation.

#### fP deposition on zymosan by plasma and fP-depleted serum

To supplement the ELISA experiments on fP deposition on the solid phase after zymosan-induced activation of NHS (Fig. 4A, 4B), similar experiments were made with fP-depleted (fPd) serum. With NHS, high OD values for fP deposition were obtained and low values with fPd serum, increasing again after reconstitution with fP (Fig. 5A). The OD value of fPd serum was statistically different ( $p < 0.05$ ) from NHS and from fP-reconstituted fPd serum ( $n = 6$ ).

To study the reactivity of zymosan in as close to physiological conditions as possible, interaction with lepirudin plasma (NHP) was studied in flow cytometry using deposition of fP and TCC as readouts. The recombinant hirudin analog lepirudin is a highly specific thrombin inhibitor and a suitable anticoagulant without adverse effects on complement in studies of the inflammatory response in whole blood and plasma (47–49). Deposition of fP on zymosan was substantial with mean fluorescence intensity (MFI) of 42 after activation of NHP (Fig. 5B, dark red curve). Compstatin inhibited the signal to MFI values identical to the isotype control (Fig. 5B, light red curve). The inhibition of fP deposition by compstatin was statistically significant ( $p < 0.0001$ ) ( $n = 6$ ). fP deposition by fPd was identical to the isotype control and increased after reconstitution with fP (Fig. 5C). The individual MFI data are given in Supplemental Table I.

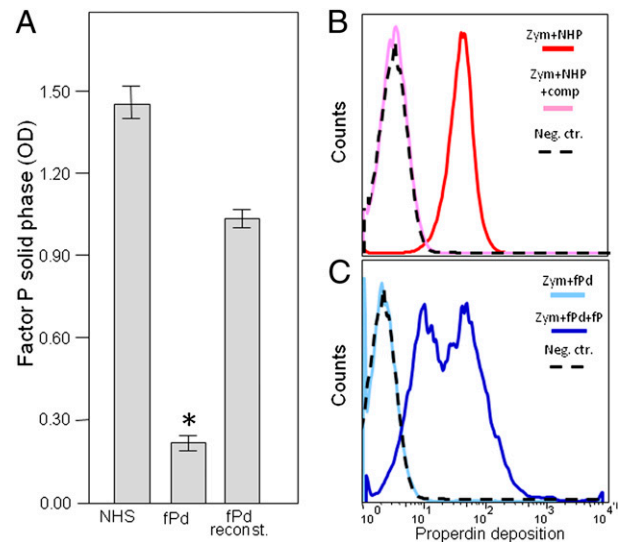


**FIGURE 5.** (A) Deposition of fP on the solid phase in ELISA after incubation of zymosan with NHS compared with fPd serum and fPd serum reconstituted with purified fP. (B) Flow cytometry showing deposition of fP on zymosan after activation of NHP (dark red curve) and inhibition by compstatin (light red curve) with isotype control in the black stippled curve. (C) Similar experiment to compare zymosan reactivity with fPd serum and fPd serum reconstituted with purified fP. \* $p < 0.05$ .

Deposition of TCC on zymosan after interaction with NHP was substantial with MFI of 336 (Supplemental Fig. 2, dark green curve). Compstatin inhibited this binding to MFI of 6.5 (Supplemental Fig. 2, light green curve). The corresponding MFI value of the isotype control was 3.9 (Supplemental Fig. 2, black stippled line), confirming C3 dependence of TCC deposition. Similar experiments with NHS gave results corresponding fully to those obtained with NHP.

#### fP deposition on *E. coli* by flow cytometry

Incubation of *E. coli* strain D31m4 with NHS induced deposition of fP on the bacteria (Fig. 6A, dark red curve), which was blocked by compstatin (light red curve), giving MFI values similar to those of the isotype control (Supplemental Table I). The inhibition of fP deposition by compstatin was statistically significant ( $p < 0.0001$ ) ( $n = 6$ ). Incubation of *E. coli* strain D31m4 with fPd serum gave an MFI value similar to the isotype control and increased after reconstitution with fP (Fig. 6B, Supplemental Table I). Similar results were found in two other *E. coli* strains (D31m3 and ED3869).

#### Deposition of fP released from human blood PMNs on zymosan and *E. coli*

Deposition of fP released from PMA-activated PMNs (PMNfP) on zymosan was studied in ELISA (Fig. 7A). No deposition of PMNfP alone was found, as the OD values were identical to the isotype control Ab. In contrast, PMNfP from this supernatant showed significant ( $p < 0.0001$ ) deposition when incubated in fPd serum. In turn, addition of compstatin inhibited this PMNfP deposition completely (Fig. 7A, Supplemental Table I), analogous to what was repeatedly observed in experiments with normal serum. Identical observations were made in flow cytometry regarding deposition of PMNfP on *E. coli* (Fig. 7B, 7C).

## Discussion

In the present study, we found that inhibition of fP binding in NHS and lepirudin plasma to zymosan and to *E. coli* by compstatin

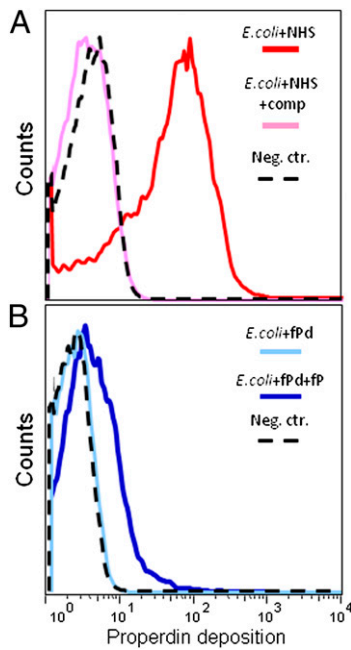


**FIGURE 6.** (A) Flow cytometry to show deposition of fP in NHS (1:2) on *E. coli* (dark red curve) and effect of compstatin (light red curve). Deposition of fP was detected by reaction with anti-fP mAb and FITC-conjugated anti-mouse IgG. Control replacing anti-fP mAb with its isotype control (stippled black curve). (B) The same layout with fPd serum in light blue and reconstitution with fP in dark blue. Similar findings in six experiments on three *E. coli* strains are shown.

served to distinguish between primary binding of fP, consistent with fP as a recognition molecule, and secondary binding to C3b initially formed in the tick-over reaction, consistent with fP as an amplification molecule. In our experiments, we consistently found that fP both from human serum and released from activated PMNs did not bind directly to zymosan or *E. coli*, but that binding of fP was dependent on initial C3b binding.

The amplification function of fP is well established, whereas a direct activation of AP by fP recognition is a present topic of investigation. The amplification function is associated with the unstable C3bBb complex in AP (10, 11) interacting with fP to form a more stable C3bBbP complex (12), with longer lasting enzyme activity essential for effective AP amplification. The dependency of CP and LP on AP amplification is similar. Thus, in our earlier study, anti-fD mAb inhibited >80% of C5a and TCC release into the fluid phase after HAIGG-induced activation of CP (24), similar to data later found for LP (25) and corresponding to recent detailed structural studies showing analogous interactions in the initiating complexes of CP and LP (50).

Evidence for the role of fP as a recognition molecule in AP started with experiments showing that purified fP bound to a bio-sensor surface could serve as a platform for in situ assembly of AP C3 convertases (9, 14). Extensive further experiments indicating that AP is initiated by noncovalent attachment of fP to a target surface (2) were performed in EGTA  $Mg^{2+}$  buffer. In this system, however, the autoactivation (tick-over) of C3 and the AP pathway amplification are intact (51–54) and would permit slow continuous C3b deposition, making it difficult to demonstrate whether fP reacts as an initial pattern recognition molecule or binds secondarily after initial C3b deposition on a reactive surface.

The authors of the studies describing properdin as a recognition molecule (2, 14) noted that purified properdin may react differently from properdin in serum owing to the tick-over reaction.

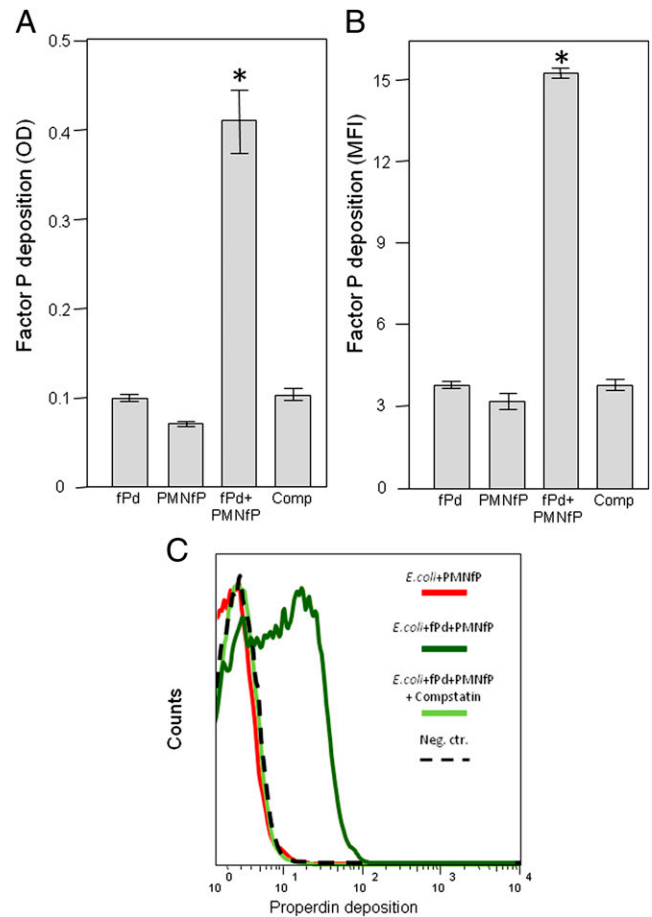


**FIGURE 7.** (A) Deposition of PMNfP on the solid phase in ELISA after incubation of zymosan with fPd serum, PMNfP, PMNfP incubated in fPd serum, and the latter inhibited with compstatin (Comp). (B) Flow cytometry showing PMNfP deposition on *E. coli* bacteria with same experimental design as described in (A). (C) Histogram from one representative experiment described in (B), showing PMNfP (red curve), PMNfP incubated in fPd serum (dark green curve), and the latter inhibited with compstatin (light green curve). The isotype control is shown (black stippled curve). \* $p < 0.05$ .

Properdin released from activated, degranulated neutrophils may also react differently from properdin in serum (15). Our data clearly indicate that plasma and serum fP and fP released from PMNs behave similarly with respect to binding to zymosan and *E. coli*. Notably, PMN-released fP did not bind unless incubated in fPd serum. Then, efficient binding took place, but it was completely abolished by compstatin, exactly as seem for serum fP.

In contrast to our findings with exogenous ligands (zymosan and *E. coli*), compelling evidence for C3-independent direct fP binding to endogenous ligands, that is, late apoptotic or necrotic cells (55), was based on a set of different, independent criteria: binding was demonstrated after incubation of the cells with purified human fP in serum-free RPMI 1640 culture medium; purified fP bound to necrotic splenocytes of C3 knockout ( $C3^{-/-}$ ) mice similar to cells from wild-type mice; and purified fP bound to necrotic cells in C3-deficient serum in EDTA-containing medium, similar to binding in NHS. The ligand involved in fP binding was studied by confocal microscopy, which confirmed that fP was colocalized exclusively with fragmented DNA exposed on late apoptotic cells. This is direct evidence for fP reactivity as recognition molecule of endogenous ligands under certain conditions.



Purified fP often forms a series of oligomers of an  $\sim 53,000 M_r$  subunit, assembling into dimers ( $P_2$ ), trimers ( $P_3$ ), tetramers ( $P_4$ ), and higher forms ( $P_n$ ), which can be separated by cation exchange chromatography and gel filtration (16). In this study, unseparated purified fP and  $P_n$  was found to bind to live Raji and Jurkat cells whereas physiological forms of fP ( $P_2$ ,  $P_3$ , and  $P_4$ ) only bound to necrotic and Jurkat cells. The live and necrotic cells were incubated with different forms of fP in HBSS for 1 h at 37°C, washed, and analyzed by FACS with an anti-fP mAb or an IgG1 mAb isotype control, followed by an FITC-conjugated anti-mouse IgG Ab. This procedure clearly indicates C3 independence of the physiological forms of fP binding to necrotic Raji and Jurkat cells.

To explore whether fP bound initially as a recognition molecule with initial activating function or participated as an amplifier of AP after initial C3b deposition, we performed inhibition experiments with the C3-reactive peptide compstatin. Compstatin was the first non-host-derived complement inhibitor shown to block the CP, LP, and AP activation pathways (26). This 13-residue cyclic peptide was discovered by a phage display, random peptide library search. Analogs with markedly increased potency (V4W, H9A) were later identified (27). These compounds bind C3, C3(H<sub>2</sub>O), C3b, and C3c with high specificity, inhibiting complement activation (56). The crystal structure of compstatin in complex with C3c has been presented (28). The compstatin binding site is formed by the macroglobulin domains 4 and 5. A model was proposed in which compstatin sterically hinders the access of substrate C3 to the convertase complexes, thus blocking complement activation and amplification (28). In the present experiments, compstatin completely inhibited fP binding to zymosan in ELISA, whereas deposition of C4b, occurring earlier in the cascade, was not inhibited. In contrast, C4b deposition was increased in the presence of compstatin, most likely due to increased availability of acceptor sites for covalent binding of C4b in the absence of C3b.

Inhibition by anti-fD was incomplete, whereas anti-fP inhibited fP deposition completely at all zymosan concentrations tested (Fig. 4A). To explain the latter distinction, an interaction of fP with C3b independent of fD would need to occur. In surface plasmon resonance spectroscopy, fP has been shown to bind strongly to C3b and C3bB without further action of fD (14), explaining the finding of complete inhibition by anti-fP.

The importance of fP reactivity in vivo has been studied in murine autoimmune models by using gene-targeted fP-deficient mice in studies of zymosan-induced arthritis (57). Furthermore, fP deficiency rescued mice from AP complement-mediated embryonic lethality caused by deficiency of the membrane complement regulator *Crry* and markedly reduced disease severity in the K/BxN model of arthritis (58). In the present in vitro studies, fP reactivity with the exogenous Ags zymosan and *E. coli*, C3b dependence was demonstrated, whereas C3b independence and direct fP activity as a recognition molecule was seen with selected endogenous Ags, such as necrotic and late apoptotic cells (16, 55), whereas Ferreira et al. (16) showed that fP bound to zymosan as well.

The reaction pattern of purified fP and fP in serum has revealed some striking differences, for example, in reaction with apoptotic T cells (15). Purified fP bound to apoptotic T cells, whereas similar binding of fP in serum to the apoptotic cells was C3-dependent. Additional experiments indicated that fP freshly released from activated, degranulating neutrophils bound to apoptotic T cells, whereas endogenous fP in serum is strictly regulated. These observations appear directly related to complement involvement in neutrophil-mediated diseases (59).

In our experiments, we included both serum and lepirudin plasma, with the latter used to get as close to physiological con-

ditions as possible. All results were comparable. Thus, we conclude that binding of fP in human serum and plasma, as well as fP released from PMNs (59, 60), to zymosan and *E. coli* was C3-dependent, indicating an initial binding of C3b followed by secondary binding of fP. Similar observations were made in another recently published study showing that fP in serum bound to glycan particles and zymosan “only in the presence of active C3” (61). In this study, the authors showed binding of fP in flow cytometry after incubation of glycan particles and zymosan in NHS in EGTA Mg<sup>2+</sup> buffer. Binding of fP was not obtained in C3-depleted serum, but in the C3-depleted serum reconstituted with purified C3. Another recent study showed that the tissue damage in an elastase-induced mouse model of abdominal aortic aneurysm depended on AP activation, being C3-dependent (62). Direct binding of purified fP as a recognition molecule has been demonstrated in other circumstances (16, 55). Our study indicates that inhibition experiments with compstatin are valuable to identify additional settings in which fP reacts as a recognition molecule.

## Acknowledgments

We thank Wenchao Song for valuable comments to the manuscript.

## Disclosures

The authors have no financial conflicts of interest.

## References

- Pillemer, L., L. Blum, I. H. Lepow, O. A. Ross, E. W. Todd, and A. C. Wardlaw. 1954. The properdin system and immunity. I. Demonstration and isolation of a new serum protein, properdin, and its role in immune phenomena. *Science* 120: 279–285.
- Spitzer, D., L. M. Mitchell, J. P. Atkinson, and D. E. Hourcade. 2007. Properdin can initiate complement activation by binding specific target surfaces and providing a platform for de novo convertase assembly. *J. Immunol.* 179: 2600–2608.
- Ecker, E. E. 1958. Louis Pillemer; 1908–1957. *J. Immunol.* 80: 415–416.
- Lepow, I. H. 1980. Presidential address to American Association of Immunologists in Anaheim, California, April 16, 1980. Louis Pillemer, properdin, and scientific controversy. *J. Immunol.* 125: 471–475.
- Lachmann, P. 2006. Complement before molecular biology. *Mol. Immunol.* 43: 496–508.
- Kimura, Y., T. Miwa, L. Zhou, and W. C. Song. 2008. Activator-specific requirement of properdin in the initiation and amplification of the alternative pathway complement. *Blood* 111: 732–740.
- Stover, C. M., J. C. Luckett, B. Echtenacher, A. Dupont, S. E. Figgitt, J. Brown, D. N. Männel, and W. J. Schwaeble. 2008. Properdin plays a protective role in polymicrobial septic peritonitis. *J. Immunol.* 180: 3313–3318.
- Harboe, M., and T. E. Mollnes. 2008. The alternative complement pathway revisited. *J. Cell. Mol. Med.* 12: 1074–1084.
- Kemper, C., J. P. Atkinson, and D. E. Hourcade. 2010. Properdin: emerging roles of a pattern-recognition molecule. *Annu. Rev. Immunol.* 28: 131–155.
- Medicus, R. G., O. Götze, and H. J. Müller-Eberhard. 1976. Alternative pathway of complement: recruitment of precursor properdin by the labile C3/C5 convertase and the potentiation of the pathway. *J. Exp. Med.* 144: 1076–1093.
- Pangburn, M. K., and H. J. Müller-Eberhard. 1986. The C3 convertase of the alternative pathway of human complement: enzymic properties of the bimolecular proteinase. *Biochem. J.* 235: 723–730.
- Fearon, D. T., and K. F. Austen. 1975. Properdin: binding to C3b and stabilization of the C3b-dependent C3 convertase. *J. Exp. Med.* 142: 856–863.
- Fearon, D. T. 1979. Activation of the alternative complement pathway. *CRC Crit. Rev. Immunol.* 1: 1–32.
- Hourcade, D. E. 2006. The role of properdin in the assembly of the alternative pathway C3 convertases of complement. *J. Biol. Chem.* 281: 2128–2132.
- Kemper, C., L. M. Mitchell, L. Zhang, and D. E. Hourcade. 2008. The complement protein properdin binds apoptotic T cells and promotes complement activation and phagocytosis. *Proc. Natl. Acad. Sci. USA* 105: 9023–9028.
- Ferreira, V. P., C. Cortes, and M. K. Pangburn. 2010. Native polymeric forms of properdin selectively bind to targets and promote activation of the alternative pathway of complement. *Immunobiology* 215: 932–940.
- Krurup, A., S. Thiel, A. Hansen, T. Fujita, and J. C. Jensenius. 2004. L-ficolin is a pattern recognition molecule specific for acetyl groups. *J. Biol. Chem.* 279: 47513–47519.
- Garred, P., C. Honoré, Y. J. Ma, S. Rørvig, J. Cowland, N. Borregaard, and T. Hummelshøj. 2010. The genetics of ficolins. *J. Innate Immun.* 2: 3–16.
- Gout, E., V. Garlatti, D. F. Smith, M. Lacroix, C. Dumestre-Pérard, T. Lunardi, L. Martin, J. Y. Cesbron, G. J. Arlaud, C. Gaboriaud, and N. M. Thielens. 2010. Carbohydrate recognition properties of human ficolins: glycan array screening reveals the sialic acid binding specificity of M-ficolin. *J. Biol. Chem.* 285: 6612–6622.

20. Harboe, M., P. Garred, M. S. Borgen, G. L. Stahl, A. Roos, and T. E. Mollnes. 2006. Design of a complement mannose-binding lectin pathway-specific activation system applicable at low serum dilutions. *Clin. Exp. Immunol.* 144: 512–520.
21. Suankratay, C., X. H. Zhang, Y. Zhang, T. F. Lint, and H. Gewurz. 1998. Requirement for the alternative pathway as well as C4 and C2 in complement-dependent hemolysis via the lectin pathway. *J. Immunol.* 160: 3006–3013.
22. Brouwer, N., K. M. Dolman, R. van Zwieten, E. Nieuwenhuys, M. Hart, L. A. Aarden, D. Roos, and T. W. Kuijpers. 2006. Mannan-binding lectin (MBL)-mediated opsonization is enhanced by the alternative pathway amplification loop. *Mol. Immunol.* 43: 2051–2060.
23. Zhao, H., N. Wakamiya, Y. Suzuki, M. T. Hamonko, and G. L. Stahl. 2002. Identification of human mannose binding lectin (MBL) recognition sites for novel inhibitory antibodies. *Hybrid. Hybridomics* 21: 25–36.
24. Harboe, M., G. Ulvund, L. Vien, M. Fung, and T. E. Mollnes. 2004. The quantitative role of alternative pathway amplification in classical pathway induced terminal complement activation. *Clin. Exp. Immunol.* 138: 439–446.
25. Harboe, M., P. Garred, E. Karlström, J. K. Lindstad, G. L. Stahl, and T. E. Mollnes. 2009. The down-stream effects of mannan-induced lectin complement pathway activation depend quantitatively on alternative pathway amplification. *Mol. Immunol.* 47: 373–380.
26. Sahu, A., B. K. Kay, and J. D. Lambris. 1996. Inhibition of human complement by a C3-binding peptide isolated from a phage-displayed random peptide library. *J. Immunol.* 157: 884–891.
27. Mallik, B., M. Katragadda, L. A. Spruce, C. Carafides, C. G. Tsokos, D. Morikis, and J. D. Lambris. 2005. Design and NMR characterization of active analogues of compstatin containing non-natural amino acids. *J. Med. Chem.* 48: 274–286.
28. Janssen, B. J., E. F. Half, J. D. Lambris, and P. Gros. 2007. Structure of compstatin in complex with complement component C3c reveals a new mechanism of complement inhibition. *J. Biol. Chem.* 282: 29241–29247.
29. Magotti, P., D. Ricklin, H. Qu, Y. Q. Wu, Y. N. Kaznessis, and J. D. Lambris. 2009. Structure-kinetic relationship analysis of the therapeutic complement inhibitor compstatin. *J. Mol. Recognit.* 22: 495–505.
30. Hourcade, D. E. 2008. Properdin and complement activation: a fresh perspective. *Curr. Drug Targets* 9: 158–164.
31. Collard, C. D., A. Väkevä, M. A. Morrissey, A. Agah, S. A. Rollins, W. R. Reenstra, J. A. Buras, S. Meri, and G. L. Stahl. 2000. Complement activation after oxidative stress: role of the lectin complement pathway. *Am. J. Pathol.* 156: 1549–1556.
32. Fung, M., P. G. Loubser, A. Undar, M. Mueller, C. Sun, W. N. Sun, W. K. Vaughn, and C. D. Fraser, Jr. 2001. Inhibition of complement, neutrophil, and platelet activation by an anti-factor D monoclonal antibody in simulated cardiopulmonary bypass circuits. *J. Thorac. Cardiovasc. Surg.* 122: 113–122.
33. Mollnes, T. E., T. Lea, S. S. Frøland, and M. Harboe. 1985. Quantification of the terminal complement complex in human plasma by an enzyme-linked immunosorbent assay based on monoclonal antibodies against a neoantigen of the complex. *Scand. J. Immunol.* 22: 197–202.
34. Seelen, M. A., A. Roos, J. Wieslander, T. E. Mollnes, A. G. Sjöholm, R. Wurznier, M. Loos, F. Tedesco, R. B. Sim, P. Garred, et al. 2005. Functional analysis of the classical, alternative, and MBL pathways of the complement system: standardization and validation of a simple ELISA. *J. Immunol. Methods* 296: 187–198.
35. Harboe, M., O. Closs, L. J. Reitan, and P. Draper. 1981. Demonstration of antibodies reacting with different determinants on *Mycobacterium leprae* antigen 7. *Int. J. Lepr. Other Mycobact. Dis.* 49: 147–158.
36. Laursen, I., G. Houen, P. Højrup, N. Brouwer, L. B. Krogsøe, L. Blou, and P. R. Hansen. 2007. Second-generation nanofiltered plasma-derived mannan-binding lectin product: process and characteristics. *Vox Sang.* 92: 338–350.
37. Garred, P., F. Larsen, H. O. Madsen, and C. Koch. 2003. Mannose-binding lectin deficiency: revisited. *Mol. Immunol.* 40: 73–84.
38. Larsen, F., H. O. Madsen, R. B. Sim, C. Koch, and P. Garred. 2004. Disease-associated mutations in human mannose-binding lectin compromise oligomerization and activity of the final protein. *J. Biol. Chem.* 279: 21302–21311.
39. Larsson, K., K. Wester, P. Nilsson, M. Uhlén, S. Hober, and H. Wernérus. 2006. Multiplexed PREST immunization for high-throughput affinity proteomics. *J. Immunol. Methods* 315: 110–120.
40. Persson, A., S. Hober, and M. Uhlén. 2006. A human protein atlas based on antibody proteomics. *Curr. Opin. Mol. Ther.* 8: 185–190.
41. Hopp, T. P., and K. R. Woods. 1981. Prediction of protein antigenic determinants from amino acid sequences. *Proc. Natl. Acad. Sci. USA* 78: 3824–3828.
42. Mollnes, T. E., T. Lea, M. Harboe, and J. Tschopp. 1985. Monoclonal antibodies recognizing a neoantigen of poly(C9) detect the human terminal complement complex in tissue and plasma. *Scand. J. Immunol.* 22: 183–195.
43. Mollnes, T. E., H. Redl, K. Høgåsen, A. Bengtsson, P. Garred, L. Speilberg, T. Lea, M. Oppermann, O. Götze, and G. Schlag. 1993. Complement activation in lepta baboons detected by neoptope-specific assays for C3b/iC3b/C3c, C5a and the terminal C5b-9 complement complex (TCC). *Clin. Exp. Immunol.* 91: 295–300.
44. Hein, E., C. Honoré, M. O. Skjøedt, L. Munthe-Fog, T. Hummelshøj, and P. Garred. 2010. Functional analysis of Ficolin-3 mediated complement activation. *PLoS ONE* 5: e15443.
45. Kjaer, T. R., A. G. Hansen, U. B. Sørensen, O. Nielsen, S. Thiel, and J. C. Jensenius. 2011. Investigations on the pattern recognition molecule M-ficolin: quantitative aspects of bacterial binding and leukocyte association. *J. Leukoc. Biol.* 90: 425–437.
46. Thomsen, T., A. Schlosser, U. Holmskov, and G. L. Sørensen. 2011. Ficolins and FIBCD1: soluble and membrane bound pattern recognition molecules with acetyl group selectivity. *Mol. Immunol.* 48: 369–381.
47. Mollnes, T. E., O. L. Brekke, M. Fung, H. Fure, D. Christiansen, G. Bergseth, V. Videm, K. T. Lappgård, J. Köhl, and J. D. Lambris. 2002. Essential role of the C5a receptor in *E. coli*-induced oxidative burst and phagocytosis revealed by a novel leprudin-based human whole blood model of inflammation. *Blood* 100: 1869–1877.
48. Lappgård, K. T., D. Christiansen, A. Pharo, E. B. Thorgersen, B. C. Hellerud, J. Lindstad, E. W. Nielsen, G. Bergseth, D. Fadnes, T. G. Abrahamson, et al. 2009. Human genetic deficiencies reveal the roles of complement in the inflammatory network: lessons from nature. *Proc. Natl. Acad. Sci. USA* 106: 15861–15866.
49. Harboe, M., E. B. Thorgersen, and T. E. Mollnes. 2011. Advances in assay of complement function and activation. *Adv. Drug Deliv. Rev.* 63: 976–987.
50. Phillips, A. E., J. Toth, A. W. Dodds, U. V. Girija, C. M. Furze, E. Pala, R. B. Sim, K. B. Reid, W. J. Schwaeble, R. Schmid, et al. 2009. Analogous interactions in initiating complexes of the classical and lectin pathways of complement. *J. Immunol.* 182: 7708–7717.
51. Lachmann, P. J., and L. Halbwachs. 1975. The influence of C3b inactivator (KAF) concentration on the ability of serum to support complement activation. *Clin. Exp. Immunol.* 21: 109–114.
52. Pangburn, M. K., R. D. Schreiber, and H. J. Müller-Eberhard. 1981. Formation of the initial C3 convertase of the alternative complement pathway: acquisition of C3b-like activities by spontaneous hydrolysis of the putative thioester in native C3. *J. Exp. Med.* 154: 856–867.
53. Pangburn, M. K., and H. J. Müller-Eberhard. 1983. Initiation of the alternative complement pathway due to spontaneous hydrolysis of the thioester of C3. *Ann. N. Y. Acad. Sci.* 421: 291–298.
54. Bexborn, F., P. O. Andersson, H. Chen, B. Nilsson, and K. N. Ekdahl. 2008. The tick-over theory revisited: formation and regulation of the soluble alternative complement C3 convertase (C3(H<sub>2</sub>O)Bb). *Mol. Immunol.* 45: 2370–2379.
55. Xu, W., S. P. Berger, L. A. Trouw, H. C. de Boer, N. Schlagwein, C. Mutsaers, M. R. Daha, and C. van Kooten. 2008. Properdin binds to late apoptotic and necrotic cells independently of C3b and regulates alternative pathway complement activation. *J. Immunol.* 180: 7613–7621.
56. Sahu, A., A. M. Soulika, D. Morikis, L. Spruce, W. T. Moore, and J. D. Lambris. 2000. Binding kinetics, structure-activity relationship, and biotransformation of the complement inhibitor compstatin. *J. Immunol.* 165: 2491–2499.
57. Dimitrova, P., N. Ivanovska, W. Schwaeble, V. Gyurkovska, and C. Stover. 2010. The role of properdin in murine zymosan-induced arthritis. *Mol. Immunol.* 47: 1458–1466.
58. Kimura, Y., L. Zhou, T. Miwa, and W. C. Song. 2010. Genetic and therapeutic targeting of properdin in mice prevents complement-mediated tissue injury. *J. Clin. Invest.* 120: 3545–3554.
59. Camous, L., L. Roumenina, S. Bigot, S. Brachemi, V. Frémeaux-Bacchi, P. Lesavre, and L. Halbwachs-Mecarelli. 2011. Complement alternative pathway acts as a positive feedback amplification of neutrophil activation. *Blood* 117: 1340–1349.
60. Wirthmueller, U., B. Dewald, M. Thelen, M. K. Schäfer, C. Stover, K. Whaley, J. North, P. Eggleton, K. B. Reid, and W. J. Schwaeble. 1997. Properdin, a positive regulator of complement activation, is released from secondary granules of stimulated peripheral blood neutrophils. *J. Immunol.* 158: 4444–4451.
61. Agarwal, S., C. A. Specht, H. Haibin, G. R. Ostroff, S. Ram, P. A. Rice, and S. M. Levitz. 2011. Linkage specificity and role of properdin in activation of the alternative complement pathway by fungal glycans. *MBio* 2: e00178-11.
62. Pagano, M. B., H. F. Zhou, T. L. Ennis, X. Wu, J. D. Lambris, J. P. Atkinson, R. W. Thompson, D. E. Hourcade, and C. T. Pham. 2009. Complement-dependent neutrophil recruitment is critical for the development of elastase-induced abdominal aortic aneurysm. *Circulation* 119: 1805–1813.